Journal of Electronics and Electrical Engineering
https://ojs.wiserpub.com/index.php/JEEE

UNIVERSAL WISER PUBLISHER

Research Article

Techno-Economic Design and Sensitivity Analysis of a DC Microgrid for a Remote Community: A Case Study in Ghana

Godfred Atinkum*, **M. Tariq Iqbal**, **John E. Quaicoe**

Department of Electrical and Computer Engineering, Memorial University of Newfoundland, St. Johns, NL, A1C 5S7, Canada
E-mail: godredatinkum14@gmail.com

Received: 5 February 2025; **Revised:** 9 April 2025; **Accepted:** 30 April 2025

Abstract: Access to electricity is crucial to human development. Many villages in Ghana remain undeveloped due to a lack of electricity. One way to increase energy access is to electrify these communities using renewable resources. Resource availability, reliability, sustainability, and cost-benefit analysis are vital in the design process. To that end, this paper presents a techno-economic design of a renewable-energy-based microgrid for an island community in Ghana using HOMER Pro. To ensure an efficient design, factors such as maximum annual capacity shortage and minimum renewable fraction are utilized as design constraints. The proposed system combines a hybrid solar-wind-diesel generator-battery-converter as the optimal system architecture. From the simulation results, the optimal component sizes are solar-102 kW, wind-24.3 kW, diesel generator-30 kW, converter-50 kW, and battery-289 kWh. The system's total annual energy production is 207,827 kWh, with a 98.6% renewable fraction and an estimated yearly CO_2 emission of 1,488 kg, making the system environmentally friendly. The reported capital, net present, and operating costs are $133,275.00, $250,689.00, and $4,696.54, respectively, at an LCOE of $0.09812. The system has a simple payback period of approximately 7 years with a 35.4% return on investment. Additionally, detailed sensitivity analyses are carried out on key variables, including fuel price, inflation, wind speed, solar radiation, and battery minimum state of charge to assess their impact on system performance. Finally, the study analyzes demand increases and load efficiency improvements to the existing system performance.

Keywords: energy access, greenhouse gas (GHG), microgrid (MG), net present cost (NPC), levelized cost of energy (LCOE)

1. Introduction

Energy access remains one of the critical challenges in rural areas in sub-Saharan Africa. According to the International Energy Agency, approximately 600 million people in the region live without electricity [1]. This situation, sometimes called 'energy poverty', hinders socio-economic development and quality of life [2]. In Ghana, it was estimated that about 14.9% of the population still lacks access to electricity, based on the World Bank report in 2022 [3]. Many of this group live in rural and remote areas, including island communities around Volta Lake. Residents in these areas rely on diesel generators and kerosene lamps to power their homes. Nonetheless, these fossil fuels not only contribute to environmental pollution but are unreliable, inefficient, and incur high operational costs. Additionally, the lack of electricity has impacted education, healthcare, access to other primary amenities, and local business investments [4]-[6]. Consequently, this situation has

DOI: https://doi.org/10.37256/jeee.4120256509

driven efforts to explore alternative and sustainable means of providing electricity to these underserved communities in Ghana.

Renewable energy solutions such as a microgrid (MG) [7] systems have emerged as viable alternatives to address the problem of rural electrification [8]-[10]. These technologies offer an opportunity to electrify off-grid communities. They are also a sustainable and cost-effective means of powering homes, schools, and small businesses. MGs can be operated as standalone systems or connected to the utility grid. In remote areas, standalone MGs are the preferred option.

The government of Ghana has implemented several key initiatives and frameworks to increase energy access in rural areas. Notable among these include the National Electrification Scheme (NES), which aimed to achieve 100% electrification in communities with a population of 500 by 2020 [11], [12]. Additionally, the Ghana Energy Development and Access Project (GEDAP), in collaboration with international partners, has made efforts to scale up renewable energy access in remote areas [13]. Despite these efforts, progress has been uneven, and many rural communities remain without electricity. To bridge this gap, research into context-specific solutions, such as the most cost-effective technologies and optimal MG configuration, is required.

Various research studies on different MG design methodologies for different applications have been recorded in literature. This section is dedicated to reviewing past research studies on these methodologies. Table 1 presents a summary of some of the prior studies in the field, highlighting objectives and system architectures.

Table 1. Review of related studies on MGs

[Ref]/Author/Year	Site location	System architecture (s)	Objective (s)	Simulation software
[14]/ M. Nurunnabi et al/ 2019	Magnama, Dinajpur, Kuakata, Sitakunka, all in Bangladesh	Grid/Wind, PV/Grid, Wind/PV/Grid, Wind/PV/Grid	To optimally design an MG system for different regions in Bangladesh and minimize system costs.	HOMER
[15]/ S. Palanisamy et al/ 2024	India	PV/Wind/Battery/ Biogas	To optimally design a hybrid system for hydrogen and EV charging	HOMER
[16] Y. Lin et al/ 2022	China	PV/Wind/Battery	Design off-grid medium voltage DC MG	PSCAD/EMTDC
[17]/ N. Alluraiah et al/ 2023	India	PV/Wind/Grid	Minimize LCOE and GHG emissions, raise renewable energy fraction	HOMER
[18]/ S. Iqbal et al/ 2022	University campus in Pakistan	PV/Battery/Grid	To design a resilient hybrid MG to reduce campus blackouts	HOMER
[19] O. Khaled et al/ 2024	University campus in Pakistan	Grid/PV/BESS	Minimize cost, maximize renewable energy fraction	HOMER

In [20], the authors designed a converter-less DC microgrid system for a rural community in Nigeria. The community consisted of 9 houses, which are located within 100 m. The design methodology was such that each household was provided with a PV and a battery storage system. All loads were connected to a 48 V DC bus. Using one house as a reference, the system was sized so that the load variation among the houses was ±10%. HOMER Pro was used to simulate the work. Results showed that the system had an average autonomy of more than two days. The analysis also revealed that for a 100 W PV panel and a 12 V, 45 Ah battery, an average household with a typical load demand of 1 kWh/day and a peak demand of 0.109 kW will require 6 PV modules and 8 batteries. Economic analysis of the proposed system revealed a total capital cost of $4,622 and a net present cost (NPC) of $33,531. However, there is little to no net present cost effect on the proposed system should the solar irradiation change by a reasonable amount.

Similarly, HOMER was used to size an MG for a health facility in Ghana [4] and a rural community in Iran [21]. In [4], the proposed system utilized an existing diesel generator, which reduced the capital cost of the MG. Economic comparison with an existing system revealed a net saving of $310,000.00. The system in [21] tested four architectures of solar, wind, diesel generator, and battery storage systems. The winning system architecture was determined to combine solar, a generator, and a BESS.

In another study [22], a hybrid MG for a remote location in Canada is modelled using the CYME software. The design methodology employed an optimization function to minimize the annual system cost while considering components' rated power and capability limits. To enhance the operation of the BESS and maintain system autonomy, its location is

determined by analyzing the total system loss and voltage profiles of the buses. Simulation results revealed that the BESS size affected DG's start-up and operation time. A larger battery size led to a shorter DG operation time.

A hybrid MG for an isolated community in Ecuador is proposed in [23]. A k-means clustering algorithm is first applied to analyze renewable resources, specifically obtaining hourly meteorological data on solar irradiance and air temperature. This data creates normalized daily statistical information to help formulate a relationship between temperature and PV panel performance. The normalized data serves as a key factor in predicting the energy output of the PV system under typical or average conditions. To design a hybrid microgrid system for the community, six operating scenarios are considered: load shedding, continuous power supply, use of BESS, generator set, generator output power reduction, and the worst-case weather conditions. To address the impact of the worst meteorological conditions on system performance, the model incorporates this normalized data to adjust PV output predictions. Finally, a mathematical programming language is employed to optimize the hybrid microgrid's components.

Using collected data on various household energy consumption, [24] designed a standalone PV system for a farm in Cairo, Egypt. To obtain the maximum power output of the PV modules, a tilt angle of 30° is employed. Battery, inverter, and charge controller efficiencies of 0.85, 0.97, and 0.85 were assumed while considering the average daily load demand of 24.676 kWh. The average daily demand is divided by the combined system efficiencies to ensure optimal sizing. The proposed system was simulated using PVSyst software using two types of panels, 450 W and 260 W. The simulation results revealed that the 450 W PV panel had a better conversion efficiency of 17.7% compared to 15.99% of the 260 W PV panel and a higher energy value produced per area. The 260 W PV panel, on the other hand, edged the 450 W PV panel in terms of power loss and unused energy.

Similarly, PVSyst is employed to size a hybrid system in [25]. The concept involved designing and integrating PV modules between wind turbines, maximizing land use, and then carrying out the performance analysis. Load flow, short circuit, and relay coordination studies were carried out in ETAP to ascertain the performance of a hybrid-solar wind plant in India.

A backup grid-connected microgrid for a residential building in India is proposed in [26]. The system consisted of PV modules with built-in inverters, lead-acid batteries, and a DG that supplied power directly to the AC bus. The design focused on optimizing the system to reduce cost and environmental emissions. Analysis revealed that operating the proposed system and the utility grid minimized total billing costs by 3.43%. Further analysis proved that while providing 23.1% of the total energy demand of the building, the system had a significantly lower operating cost when compared to the utility. The authors also did a comprehensive study on the effect of the proposed system on the environment. The simulation revealed that operating the system off-grid produced 1,799.54 kg/yr of greenhouse gas due to the DG.

In [27], the authors modeled and analyzed the effect of roof orientation on roof-mounted PV performance. First, five roof designs and orientations, including flat, shed, sawtooth, hip, and gable roofs, were modeled using Energy 3D software. The system advisor model (SAM) is employed to size and design solar panels for each roof orientation. It was observed that the flat and shed roof orientations achieved maximum performance (energy yield) with a utilization factor of 0.892 due to the single-slope design, which accommodated many south-facing PV panels. The research, however, is limited to single buildings and did not include various cost analyses.

DC MGs are gaining much attention due to their advantages over their AC counterparts [28], [29]. Several articles have explored DC MG design [30]-[37]. Different methodologies, including simulation-based [30], [37], optimization-based [35], [36] and hybrid [38] methodologies, have been employed to plan, model, and design DC MGs. The simulation-based methodologies often use software, including HOMER and MATLAB, to size components and conduct dynamic analyses to ascertain the system's performance under varying conditions. Studies that mainly focus on minimizing system costs often use optimization techniques like mathematical programming and metaheuristic algorithms. However, optimization-based approaches require more expertise and consume many computational resources. The hybrid methodologies often combine the two approaches. In such cases, the typical approach involves sizing the system first, followed by dynamic simulation to validate its performance. These studies have examined various aspects, including system architecture, control strategies, and energy management [29]. Despite its high NPC, reference [39] used a life cycle assessment and social acceptance to justify optimizing an off-grid system.

Regional factors significantly influence the choice of system configurations, with certain system designs dominating specific geographical areas [40]. For instance, studies in tropical regions often prioritize PV/wind-based systems [17]. Conversely, investigations in subtropical regions favour biomass, micro-hydro, PV, and wind MGs [39]. In temperate regions, marine-based systems tend to be more prevalent [40].

Reference [30] argues that MATLAB/SIMULINK is more flexible in modifying optimization rules than Homer. It further suggests that the designed system could save 51% of electricity costs. However, several other studies have extensively evaluated the capabilities of HOMER in optimizing hybrid energy systems, particularly in terms of cost-effectiveness and reliability. For instance, [32], [34] demonstrated Homer's efficiency in determining optimal hybrid system configurations in Ghana by considering multiple objectives. In [31], a power system conditioner (PCS) controls power from the DC MG to the AC loads and the battery storage system. To minimize land utilization, the designed system consists of PV panels, PCS, and battery storage, all mounted on a pole. The proposed system in [31] may not be applicable in regions prone to high winds and storms due to mechanical stress and structural instability.

Until the development of the IEEE P2030.10/D12 draft standard, there were uncertainties in the specific applications of DC MGs to remote locations. Current research in using HOMER to size and design DC microgrids (MGs) for remote and island communities tends to focus on isolated case studies where the emphasis is placed on either technical performance, economic feasibility, or a combination of both. However, these studies often adopt a narrow perspective, overlooking comprehensive models that consider dynamic load conditions. There is limited research and analysis on (1) how varying load levels and (2) appliance efficiencies could impact system performance and cost during the component sizing stage of DC MGs for remote applications. Reference [30] explored different generations and load scenarios using standard and highly efficient loads. However, their analysis did not extend to cases where an existing DC microgrid (MG) incorporates highly efficient loads after being designed and operational. Furthermore, they did not evaluate the effects of such integration on critical parameters like excess generation, cost, and overall system performance.

To that end, this work seeks to design an MG tailored to the specific needs of an island community. By analyzing energy needs and evaluating potential renewable resources, this study aims to contribute to developing scalable and adaptable solutions that can accelerate rural electrification in Ghana. This study seeks to make the following contributions:

- To develop a tailored MG design for the specific energy needs, renewable resources, and geographic constraints in one of Ghana's island communities
- To perform a cost-benefit analysis to determine the best solution for rural electrification, balancing economics and environmental impact.
- To conduct a holistic sensitivity analysis on the effect of uncertainties in key variables on the proposed system.
- The study will further (1) model multiple load levels and (2) implement efficiency packages to assess how the proposed system responds to changes in load levels, seasonal load variations, and user behaviour.

The rest of this paper is organized as follows: Section 2 discusses the study area. It includes a brief description of the site, available resources, and the estimated energy consumption. The components modeling and selection criteria are presented in Section 3. Section 4 discusses the system's cost parameters, while the simulation, results, and discussion are presented in Section 5. Figure 1 illustrates the sequential steps carried out in this study.

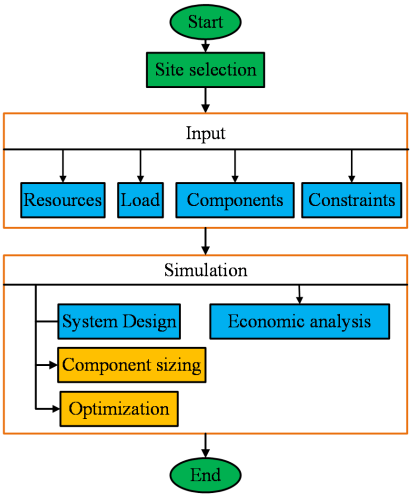

Figure 1. Azizakpe island

2. Brief description of the study area

Azizakpe, an island community in the Ada East district of the Greater Accra region of Ghana, is the location for this study. The community is situated on the Volta Lake at a latitude of 5°46′39.6″N and a longitude of 0°39′48.9″E. Azizakpe is home to a population of about 590 people [41]. Farming, fishing, and related activities serve as the major occupations in this community. Azizakpe has abundant renewable energy potential that can be harnessed to produce electricity to serve the community. Figure 2 shows a satellite view of the site obtained from Google Earth.

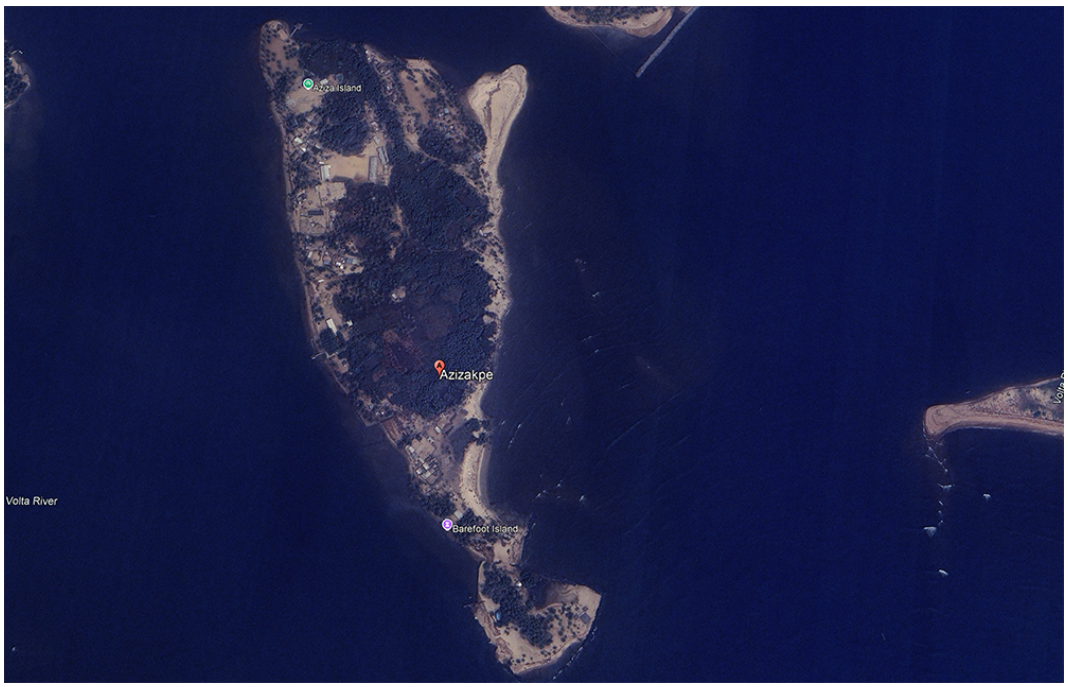

Figure 2. Proposed methodology's flow chart

2.1 *Resources*

The average monthly global horizontal irradiance (GHI), temperature, and wind data for the selected site were obtained from the National Renewable Energy Laboratory (NREL) and NASA using HOMER Pro. They are used as inputs for the PV and wind systems. A table showing the monthly average GHI, temperature, and wind speed data for the selected site is shown in Table 2. Figure 3 illustrates the average monthly insolation and wind speed for Azizakpe over a one-year period. It is observed in the table that the annual average daily radiation, temperature, and wind speed are 5.06 kWh/m^2/day, 26.65 °C and 4.79 m/s respectively. This shows that the selected location has a strong potential for PV and wind energy generation.

Table 2. Site's resource data

Month	Solar GHI (kWh/m^2/day)	Clearness index	Temperature (°C)	Wind (m/s)
January	5.026	0.534	27.420	4.060
February	5.361	0.538	27.990	4.700
March	5.548	0.534	28.060	5.010
April	5.528	0.531	27.810	4.900
May	5.107	0.505	27.300	4.520
June	4.907	0.496	26.120	5.090
July	4.735	0.575	24.800	5.860
August	5.088	0.497	24.400	5.930
September	5.202	0.504	25.130	5.460
October	5.641	0.564	26.090	4.520
November	5.726	0.604	27.130	3.770
December	5.116	0.556	27.550	3.640

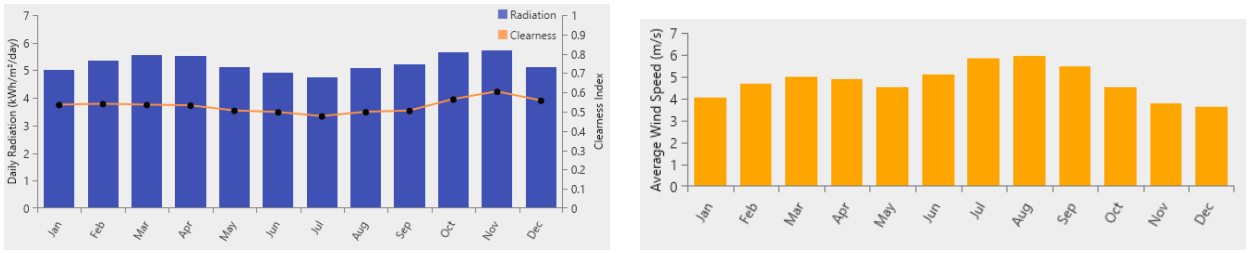

(a) (b)

Figure 3. Monthly average (a) solar and (b) wind data

2.2 *Electricity usage estimate per household*

For economic and cultural reasons, air conditioning, home heating elements, and electric cooking appliances are uncommon in a typical rural Ghanaian home. Although Ghana, located in the tropical zone, is generally warm throughout the year, most Ghanaians rely on the more affordable electric fans instead of air conditioners. Additionally, heating systems are not required in Ghanaian homes as the country does not experience extreme cold weather conditions. Many rural Ghanaian homes use traditional cooking methods encompassing charcoal, firewood, and gas stoves. Electric cookware, while convenient, is not available to prepare traditional Ghanaian meals. Hence, the typical rural Ghanaian households stick to firewood, charcoal, and, to some extent, gas stove cooking methods for cultural and economic reasons. Notwithstanding, the appliances that contribute to daily power consumption in a typical rural Ghanaian home include lights, refrigerators, television sets, electric irons, and electric fans. Furthermore, a 2019 study on appliance ownership and electricity consumption determinants was conducted in Tema, one of Ghana's big cities [42]. The study determined that the average annual energy demand per household ranged from 384 kWh to 12,578 kWh in the city. Lighting, refrigeration, air conditioning, television, and fans were identified as the primary contributors to the demand, collectively accounting for 85%. However, it should be noted that appliances such as air conditioners, washers, and refrigerators are considered

a luxury of convenience in a typical Ghanaian rural home. As such, the average energy demand per household in the main cities is much higher than in rural areas. Using the foregoing benchmark and surmise, the table below estimates a household's average daily electricity consumption in Azizakpe. The average daily energy consumption per household is estimated to be 2.5 kWh/day. The hourly variation in appliance use is based on the study in [42]. Table 3 provides an estimate of electricity consumption and load contributed by typical household appliances in Azizakpe.

Table 3. Average household load estimation by appliance usage

Equipment	Average rating (kW)	Average number per household	Hours of use per day	Average energy demand (kWh/day)
Light bulb	0.01	5	6	0.3
Television set	0.05	1	8	0.4
Fan	0.017	2	8	0.3
Refrigerator	0.1	1	12	1.2
Electric iron	1.2	1	0.25	0.3

3. Components modeling

3.1 *Solar PV system*

Ghana has abundant solar resources that can be utilized to produce both on- and off-grid electricity. A PV system is used to convert solar energy into electricity. The PV array is sized to meet the energy requirements of the household. The output power of the PV, as a function of solar irradiation, is obtained by using Equation (1) [18] below:

$$P_{PV} = P_{STC} f_{dirt} \frac{G_h(t)}{G_h(t),_{STC}} [1 + \alpha_P (T_C(t) - 25)] \quad (1)$$

where P_{STC} is the solar PV's output capacity (kW) under standard test conditions, f_{dirt} is the panel's derating factor. It accounts for the panel's performance degradation due to dirt accumulation and aging. G_h is the global horizontal irradiation in kWh/m^2/day, $G(h)_{\mathrm{STC}}$ is the standardized global horizontal irradiation. This is usually set at 1 kWh/m^2. α_P is the power temperature coefficient in %/°C and T_C is the PV cell temperature at a given time. The PV's cell temperature is assumed to be 25.

This study employs the Jinko JKM 350M-72 solar panel. Table 4 below shows the detailed characteristics of the module.

Table 4. Detailed characteristics of the PV module used in this study

PV parameter	Value
Manufacturer	Jinko solar
Model	JKM350M-72
Rated capacity (maximum power)	350 W
Voltage at maximum power	39.1 V
Current at maximum power	8.94 A
Open circuit voltage	47.5 V
Short circuit current	9.38 A
Temperature coefficient	−0.4090/°C
Operating temperature	44.9 °C
Efficiency	18%
Derating factor	85%
Capital cost	$342/kW
Replacement cost	$214/kW
O&M cost	$5/year
Lifetime	25 years

3.2 *Wind turbine*

In this study, Equation (2) is used to determine the wind turbine output power per unit area swept by the turbine blades [43], [44].

$$P_{WT} = \frac{1}{2}\rho v^3 C_P A_{rotor} \tag{2}$$

In (2), ρ is the density of the air, v is the average wind velocity, C_P is the turbine power coefficient and A_{rotor} is the rotor blades' swept area. Because the blades move in a circular motion, the swept area, $A_{rotor} = \pi r^2$ where r is the radius of the blade. The air density is calculated using the following formula: $\rho = \frac{P}{RT}$ where P is the air pressure in Pa, R and T respectively are gas constant in J/kg/K and ambient temperature in K.

According to NASA's Prediction of World Energy Resource (POWER), the average monthly wind speed for the selected site is 4.9 m/s. This study employs the Zhejiang Huaying wind turbine with a cut-in speed of 3 m/s. Detailed data on the wind turbine are tabulated in Table 5.

Table 5. Detailed characteristics of the wind turbine module used in this study

Turbine parameter	Value
Manufacturer	Zhejiang huaying
Model	HY5-AD5.6
Rated power	4.85 kW
Rotor diameter	5.6 m
Cut-in wind speed	3 m/s
Survival wind speed	50 m/s
Hub height	30 m
Capital cost	$7,178.00
Replacement cost	$3,589.00
O&M cost per unit	$100.00/year
Lifetime	20 years

3.3 *Battery energy storage system (BESS)*

A battery energy storage system is needed to store energy for use during surge times [45], and times when the other microgrid components do not output power. The BESS, therefore, improves the reliability, dependability, and capacity of the MG system. The battery should be sized to hold the load autonomously for a sufficiently longer period. Equation (3) below shows that the depth of discharge, round-trip efficiency, and the number of autonomy days affect the battery capacity.

$$C_B = \frac{E_L \times AD}{d_O d \times \eta_{inv} \times \eta_b} \tag{3}$$

It is seen from Equation (3) that the required capacity of the battery depends on the load energy, E_L, the desired days of autonomy, AD, the battery depth of discharge, $d_o d$, the battery's efficiency, η_b, and the efficiency of the inverter, η_{inv}, to adjust for losses. The BAE Secura 12 V solar battery is employed in this work. It has a maximum capacity of 201 Ah and maximum charge and discharge currents of 68.4 A and 342 A, respectively, at a round-trip efficiency of 85%. It has a lifetime of 18 years. The battery has a capital, replacement, operation, and maintenance cost of $400.00, $240.00, and $10.00, respectively.

3.4 *Converter*

A converter is needed in this study to convert the DC output voltage from the solar PV and BESS systems to AC to feed the load. Its efficiency is given as a ratio of the output power, P_{out}, to the input power, P_{in}, according to Equation (4)

$$\eta_{inv} = \frac{P_{out}}{P_{in}} \tag{4}$$

Satcon Technology's PVS-50 converter is utilized to perform the power conversion in this study. It is a 50 kW 240 V converter with inverting and rectifying efficiencies of 95.5% and 100%, respectively. It has an estimated lifetime of 15 years. The converter's capital, replacement, and O&M costs are $6,092.00, $3,655.00, and $5.00, respectively.

3.5 *Diesel generator (DG)*

This study employs a DG to complement the performance of PV and wind systems. The DG is sized to serve as a backup power supply and help meet peak demand if necessary. The equation below models the general fuel consumption of a DG based on its output power [18]:

$$F_{cons} = a.P_{DG} + b.P_{DG,rated} \tag{5}$$

P_{DG} is the hourly power generated by the DG in kW, $P_{DG,rated}$ is the hourly DG-rated capacity, a and b are coefficients in litre/kW. The cost parameters used for this model are listed in Table 6.

Table 6. DG cost parameters

DG parameter	Value
Initial capital	$8,528.78
Replacement cost	$5,118.00
O&M	$0.6/operating hour
Fuel cost	$0.95/litre
Lifetime	15,000 h

4. Cost analysis

The NPC is defined as the sum of all the project expenses over the system's life span, less the value of the incomes earned during the project's life expectancy. In this work, the net present cost comprises capital, replacement, and operational and maintenance expenses over the project's lifetime. The following equation gives the net present cost (NPC) of the project [44]:

$$NPC = \frac{C_{annual}}{CRF\,(i,\ R_{proj})} \tag{6}$$

where C_{annual} is the total annual cost ($), CRF is the capital recovery factor, i is the interest rate and R_{proj} is the project's lifetime. The CRF, used to determine how much should be earned annually to recover investments, is given by [44]:

$$CRF = \frac{i(1+i)^{N}}{(1+i)^{N}-1} \tag{7}$$

where N is the total number of years after which it is expected to recover the capital.

The HOMER software computes the cost of energy (COE), expressed in \$/kWh during the lifetime of the project, according to Equation (8) below [44], [46]:

$$COE = \frac{C_{annual}}{E_L} \tag{8}$$

where E_L is the electrical load in kWh.

The levelized cost of energy determines the mean cost per unit kWh produced. LCOE determines the viability of the proposed project and whether it will break even. It is given by [47]:

$$LCOE = \frac{\text{Total Lifetime cost}}{\text{Total Lifetime Energy}} \tag{9}$$

where the total lifetime cost will equal the sum of total annual costs over the project's estimated lifetime, and the total lifetime energy will equal the expected total energy output from the system.

5. Simulation, results, and discussions

The main objective of this study is to optimally design a system that meets the energy needs of the Azizakpe community. The project's optimal design, economic analysis, and simulations are carried out using version 3.17.1 of the Homer Pro Microgrid Analysis Tool. As seen in Figure 4, solar PV and wind turbines are added as components of the MG system due to the site's availability of resources. In addition, a battery storage device and a diesel generator are added to serve as backup power supplies. A converter converts the DC output from the components to feed the AC load. The "Homer Optimizer" feature is enabled for all the components except the converter and the diesel generator. This optimization feature allows HOMER to select the search space's optimum upper and lower limit values. In the case of the converter, the search space feature is utilized, and the converter's capacity is strictly set to 50 kW. The "simulate system with and without this generator" feature is enabled for the generator.

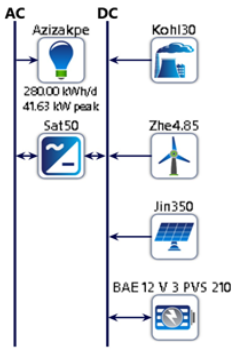

Figure 4. Proposed system architecture

Several key constraints are applied during the design process to guarantee the system's reliability, functionality, and practicality. These include a maximum annual capacity shortage of 0%, a minimum renewable fraction of 80%, and an operating reserve of 5% of peak load and 5% of the load in the current time step. Additionally, to maximize the use of renewables, the solar PV system supplies 80% of the reserve.

The simulation was carried out with 2,086 possible solutions. Of this number, 751 were infeasible due to the capacity shortage constraint, and 336 were infeasible due to the renewable energy fraction. 108 possible solutions were omitted due to the system lacking a converter or no generation sources.

5.1 *Technical analysis*

Economic indicators, including NPC, LCOE, and O&M, were utilized to select the optimal MG model. Based on the site's available resource data, the optimal system configuration is selected by prioritizing the system with the least NPC while achieving a high renewable fraction. From the simulation results, the winning system architecture is an MG system featuring PV panels, wind turbines, a DG, a converter, and a BESS. Table 7 gives a summary of individual components' capacity, energy production, and the estimated number of components required to achieve the said capacity. The total estimated energy production in a year is 246,513 kWh.

Table 7. Summary of electrical energy results

Production				
Component	Capacity	Energy production (kWh/yr)	Percent production (%)	Number of components
PV	102 kW	153,373	73.80	292
Wind turbine	24.3 kW	52,978	25.50	5
DG	30 kW	1,475	0.71	1
Consumption				
Load type		Capacity (kWh/yr)		Percentage
AC primary load		102,198		100
DC primary load		0		0%
Deferrable load		0		0%
Power supply gaps				
Quantity		Capacity (kWh/yr)		Percentage
Excess electricity		94,707		45.6%
Unmet electrical load		1.72		0.0017
Capacity shortage		10.5		0.0103
Renewable metrics				
Quantity			Value	
Renewable fraction			98.6	
Max renewable penetration			1,689	

The PV system achieves a penetration level of 150%. With a capacity factor of 17.2%, its minimum and maximum output power stand at 0 kW and 89.6 kW respectively. The mean PV output is 420 kWh/day with 0 kWh clipped production. Complementing the PV system is the wind turbine, with a penetration level of 51.8% and a capacity factor of 24.9%. Its minimum, mean, and maximum outputs are 0 kW, 6.05 kW, and 23.8 kW, respectively. The electrical production from the DG is 1,475 kWh/year at 0.561% capacity factor. The DG uses the load-following dispatch strategy to supply power to the load. Figure 5 shows each component's output power profile. Figure 5a,b shows that the respective energy profiles of both the wind and PV roughly follow the bell distribution curve, with their output powers peaking around midday. As observed in Figure 5c, the DG's output power remains nearly zero over the 12 months. This confirms that the DG is designed to operate only during peak demand periods. The monthly and hourly time series electric production data are shown in Figures 6 and 7 respectively.

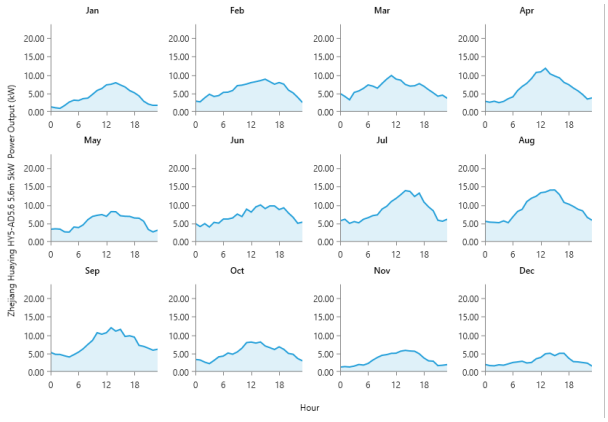

(a)

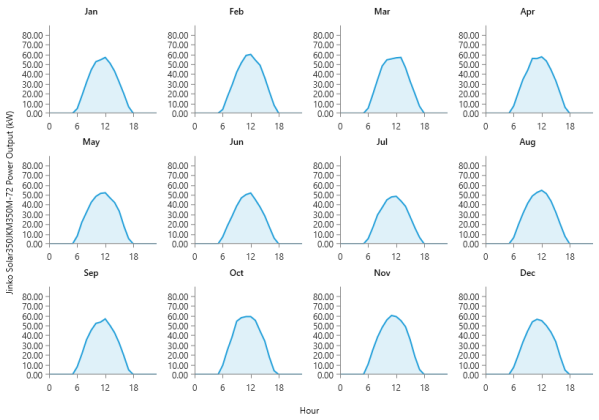

(b)

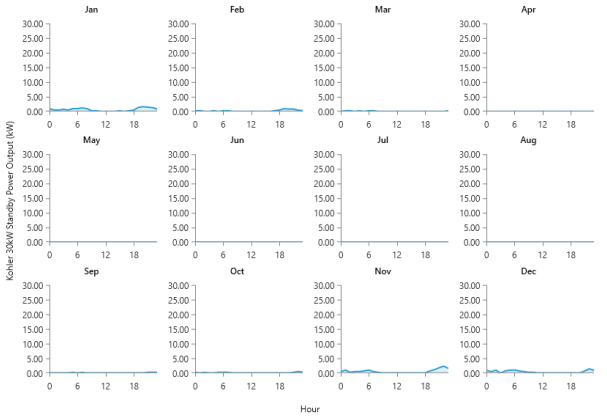

(c)

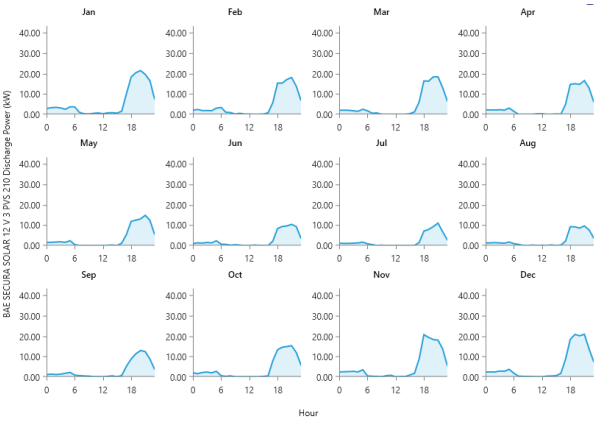

(d)

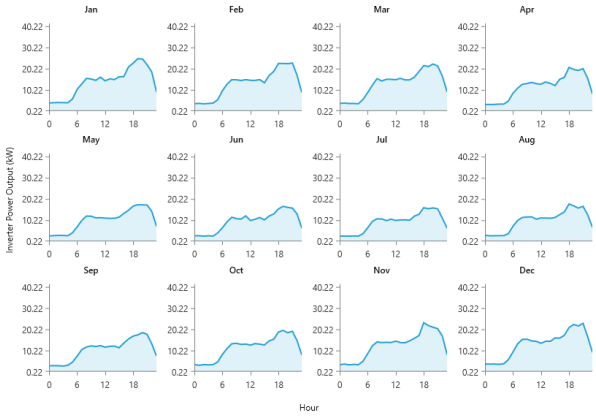

(e)

Figure 5. Profile of power flow of (a) wind turbine, (b) PV, (c) DG, (d) BESS, (e) Inverter

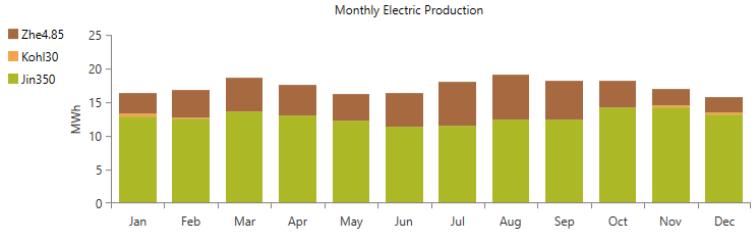

Figure 6. Monthly electric production

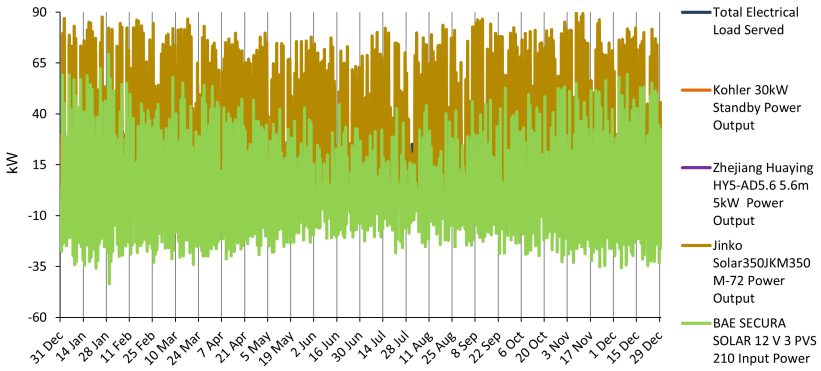

Figure 7. Cash summary of the proposed system

In addition to the energy generation equipment, the simulation results show that a system configuration with 120 battery units achieved an annual throughput of 38,687 kWh. The BESS utilized a total accessible capacity of 232 kWh from a nominal capacity of 289 kWh. The energy flow from the BESS is such that it starts producing at around 16:00, peaks at approximately 19:00, and stops producing after 06:00 hours (Figure 5d). The batteries are connected in four parallel strings of thirty units each, bringing the system voltage to 360 V. The converter in the system has a mean output of 11.7 kW, demonstrating its role in the system's optimal performance. It has a capacity factor of 23.3%. The annual losses in the converter stand at 4,816 kWh/year. In Figure 5e, the inverter outputs a nearly constant power from 06:00 h to around 18:00, with peak output power after 18:00. This indicates a higher demand for energy around this period.

5.2 *Financial analysis*

The system's economic feasibility was evaluated using financial metrics, including NPC, LCOE, capital expenditure, and O&M cost. Table 8 summarizes the proposed system's net present cost. The project's NPC is $250,689.00, with an initial investment cost of $133,275.00. Its O&M cost is $4,696.54, and LCOE is $0.09812. The BESS alone accounts for more than half (52.3%) of the system's NPC due to its relatively shorter life span of 8.78 years. This necessitates multiple replacements over the project's 25-year lifespan. Additionally, the BESS incurs relatively higher O&M costs than the other components. All these factors have contributed to its higher NPC. The PV, wind turbine, DG, and converter contribute 18.9%, 17.1%, 8.16%, and 3.45% to the system's NPC. The proposed system has a simple payback period of 7 years at a 29.4% internal rate of return and a 35.4% return on investment. Its present and annual worth are $30,795.00 and $1,232.00, respectively. The system's annualized cost is summarized in Table 9.

Table 8. Net present cost

Component	Capital ($)	Replacement ($)	O&M ($)	Fuel ($)	Salvage ($)	Total ($)
PV	34,764.57	0.00	12,706.25	0.00	0.00	47,470.82
Wind turbine	35,890.00	17,945.00	2,500.00	0.00	−13,458.75	42,876.25
DG	8,528.78	0.00	2,280.00	13,479.11	−3,821.44	20,466.45
Converter	6,092.00	3,655.00	125.00	0.00	−1,218.33	8,653.67
BESS	48,000.00	57,600.00	30,000.00	0.00	−4,378.33	131,221.67
System	133,275.35	79,200.00	47,611.25	13,479.11	−22,876.85	250,688.85

Table 9. Annualized cost

Component	Capital	Operating	Replacement	Salvage	Resource	Total
Battery	$1,920	$1,200	$2,304	−$175.13	$0.00	$5,249
PV	$1,391	$508.25	$0.00	$0.00	$0.00	$1,899
DG	$341.15	$91.20	$0.00	−$152.86	$539.16	$818.66
Converter	$243.68	$5.00	$146.20	−$48.73	$0.00	$346.15
Wind	$1,436	$100.00	$717.80	−$538.35	$0.00	$1,715
System	$5,331	$1,904	$3,168	−$915.07	$539.16	$10,028

The DG operates for 152 h annually, with approximately 52 starts within the same period. Based on this, its operational life is estimated to be 98.7 years. The fixed generation and marginal generation costs of the DG are $1.46/h and $0.312/kWh respectively. The DG consumes 568 liters of fuel with a mean electrical efficiency of 26.4%. The PV system operates for 4,380 h annually at an LCOE of $0.0124/kWh over its operational lifespan. Similarly, the wind turbine operates for 6,982 h. Its LCOE is $0.0324/kWh. With an estimated lifespan of 8.78 years, the BESS incurs a storage wear cost of $0.092/kWh. The battery system can provide up to 19.8 h of autonomy, ensuring reliable backup during low-generation periods.

5.3 *Sensitivity analysis*

Power production from renewable sources is affected by weather patterns. This means that output power fluctuates due to seasonal changes and the time of day. Additionally, inflation is a variable economic parameter that affects the system's cost. This study performs a sensitivity analysis to understand how changes in the intermittency of renewable resources and inflation affect the system's overall performance and cost. The variables considered in this context are the inflation rate, GHI, wind speed, diesel fuel price, and battery state of charge (SoC). Each variable, except the battery's SoC, is adjusted ±20% of its base value to assess how changes within this range influence the system's outcomes. The minimum SoC is varied between 0%, 20%, and 50%.

Generally, increasing the wind speed from 3.83 m/s to 5.75 m/s while keeping the other two variables constant reduces the system's fuel consumption per year, LCOE, operating cost, and NPC. Conversely, the renewable fraction of the system increases as the wind speed increases.

Increasing the GHI penetration reduces the number of wind turbines. This, in turn, reduces the system's corresponding LCOE and NPC. In a similar vein, higher inflation rates correspond to a lower COE. However, the system's NPC increases as the inflation rate increases. This is largely attributed to the high capital and O&M expenditure as the inflation rate rises. Figure 8 summarizes the effect of the inflation rate on COE and O&M costs.

Figure 9 shows the effect of the inflation rate on the NPC, daily energy production from solar, and the renewable fraction of the system. It is observed in Figure 10 that although a higher inflation rate generally corresponds to a higher renewable fraction, it comes at a cost of higher NPC. The optimum inflation rate where the best trade-off between NPC, renewable fraction, and daily solar production is shown to be between 8% and 8.8% in Figure 9.

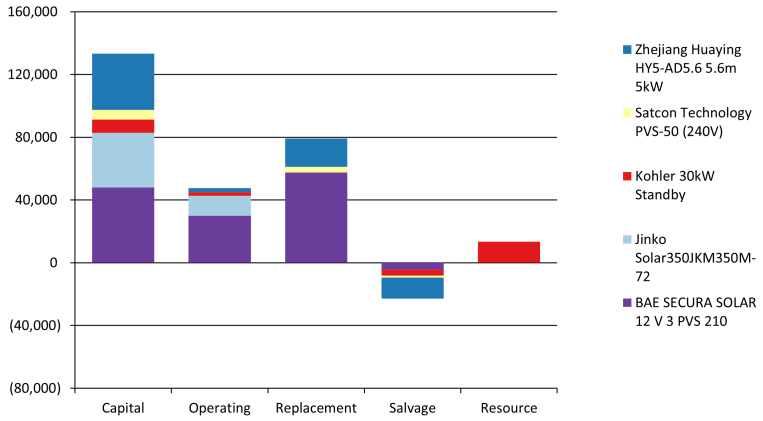

Figure 8. Effect of inflation rate on COE, O&M cost at 5.25 kWh/m^2/day and 4.79 m/s

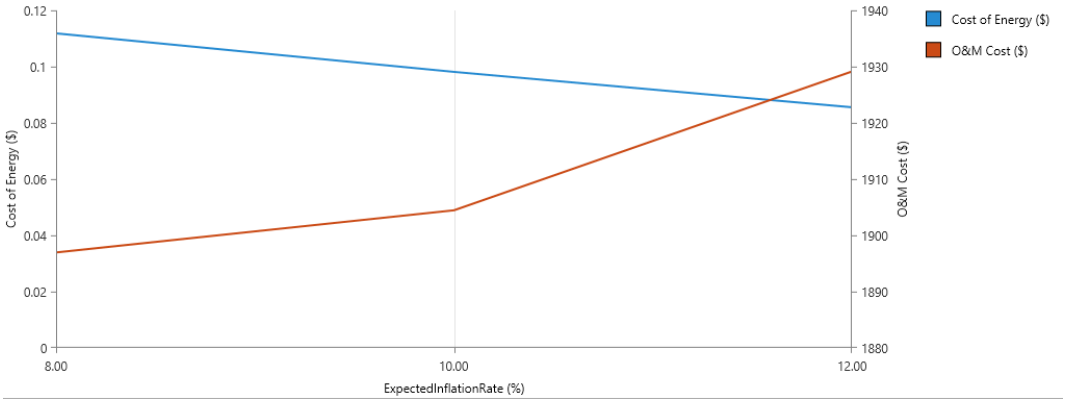

Figure 9. Surface plot of NPC with renewable fraction superimposed

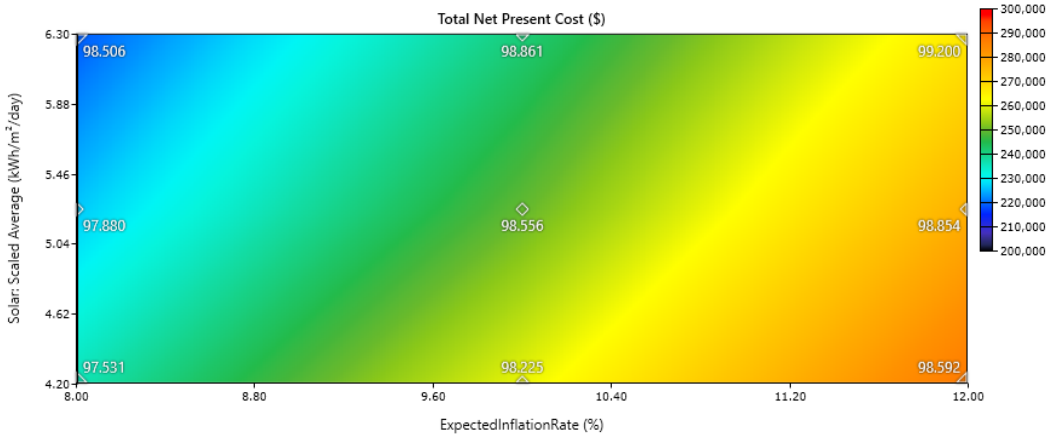

Figure 10. Effect of battery depth of discharge on storage capacity

The BESS depth of discharge affects its nominal capacity and the overall cost of the project. A 0% minimum state of discharge translates to a lower required nominal capacity. At the same time, its O&M costs and, hence, the system's NPC remain low. However, completely discharging reduces the battery's efficiency and lifetime. Maintaining a higher minimum SoC requires a higher battery capacity to compensate for the restricted usable energy. In Figure 11, as the minimum SoC is

increased from 0%, the O&M cost increases proportionally. Up until a 20% minimum SoC, the NPC increases gradually. Beyond the 20%, the NPC increases at a fast rate. The higher O&M and NPC are due to the increased BESS capacity at a higher minimum SoC.

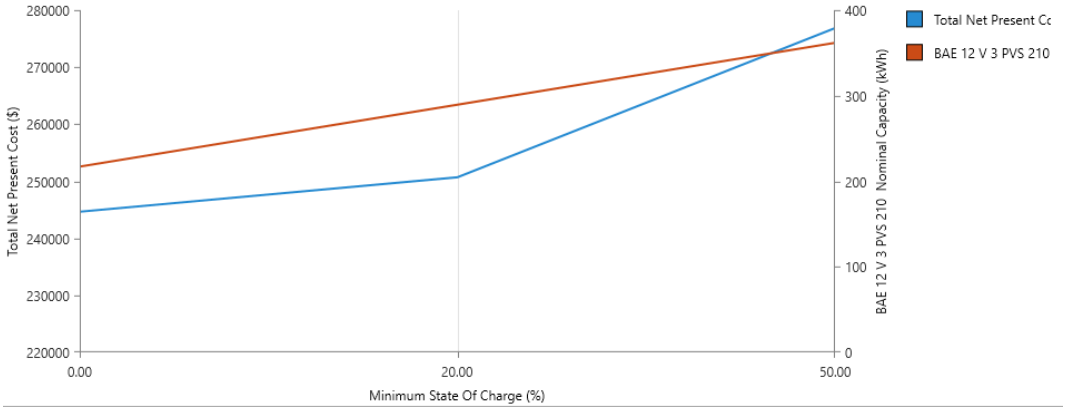

Figure 11. Effect of fuel price and inflation on battery production and NPC

An additional study is conducted on the relationship between fuel price, inflation, BESS capacity, and NPC. Because DG and BESS serve as backups, fuel prices and inflation rates directly impact the BESS's annual throughput. Figure 12 below is a surface plot of NPC with BESS annual throughput superimposed. As the inflation rate increases, the BESS annual throughput in kWh decreases. For example, at an inflation rate of 8%, the BESS annual throughput is 40,973.22 kWh.

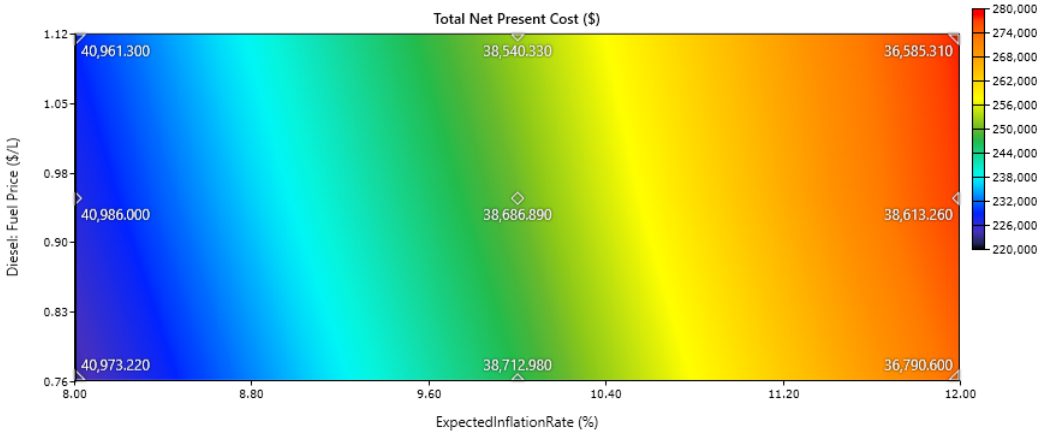

Figure 12. Effect of fuel price and inflation on battery production and NPC

However, at a 12% inflation rate, the annual throughput reduces to 36,790.6 kWh. The BESS annual throughput barely changes when the fuel price is increased from \$0.76/L to \$0.98/L. Again, system NPC increases from \$0.76/L to \$1.12/L. In addition, when the inflation rate and fuel price are increased, as seen in the top right corner of Figure 12, the BESS annual throughput is further decreased.

It should be noted that the NPC's increment or decrement is directly proportional to changes in operating cost when fuel cost and inflation rate are changed. This trend shows that the NPC is sensitive to variations in fuel price and inflation rate, with operating costs being the primary driver of these changes. As fuel prices and inflation rates increase, the cost

of maintaining system operations rises, leading to a corresponding increase in NPC. Conversely, lower fuel prices and inflation rates reduce operating costs and NPC. The foregoing analyses show that optimizing the balance between fuel costs, inflation, and battery usage is essential to maintain cost-effectiveness and system longevity.

5.4 *Environmental impact*

Sustainable design principles were a key consideration throughout the system sizing process. As such, environmental performance metrics were prioritized when evaluating different system architectures alongside technical and economic criteria. Table 10 and Figure 13 describe the system's projected greenhouse gas emissions and renewable proportion, respectively. Table 10 shows that the proposed system produces 1,488 kg of CO_2 per year. The system's emission profile is mainly due to the DG. Although the DG is the primary source of emissions, its limited operation as a backup power source or during peak demand helps minimize its environmental impact. This design approach ensures that the DG runs only when necessary, reducing fuel consumption and emission levels compared to continuously operating diesel-powered systems. This makes the system almost 100% renewable (Figure 13). Additionally, a comparison of emission factors between similar systems in Table 11 shows that the proposed system is significantly cleaner and more sustainable.

Table 10. Annual GHG emissions from the proposed system

Gas	Quantity emitted (kg/year)
Carbon dioxide	1,488
Carbon monoxide	8.11
Nitrogen oxide	7.62
Sulfur dioxide	3.64
Particulate matter	0.486
Unburned hydrocarbons	0.409

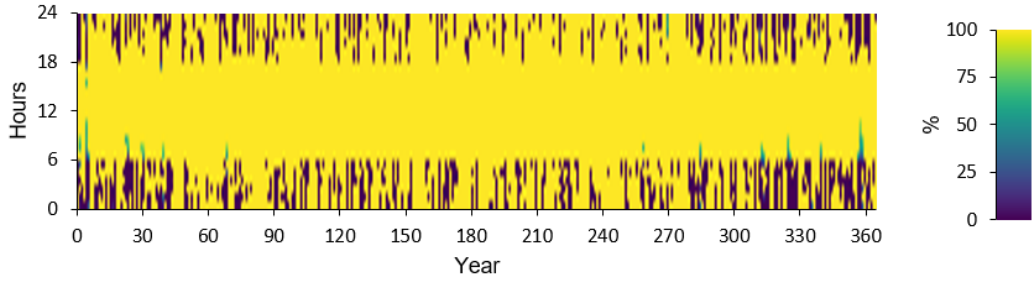

Figure 13. Instantaneous renewable output percentage of total generation

Table 11. Comparison of the proposed system to similar studies

Systems	Proposed system	[34]	[17]	[48]	[21]
Site location	Ghana	Ghana	India	Nigeria	Iran
System architecture	PV/Wind/BESS/DG	PV/BESS/DG	PV/Wind/Grid	Hydro/PV/Wind/BESS/DG	PV/BESS/DG
Energy production (kWh/year)	207,827	108,535	3,069,557	1,556,584	20,847
NPC ($)	250,689	296,552	6.92 M	1.01 M	3,224
COE ($/kWh)	0.09812	0.399	0.0751	0.106	0.371
Renewable fraction (%)	98.6	40	94	77.4	89
CO_2 emissions (kg/year)	1,488	40,362	27,153	226,386	-
E.F (kg/kWh)	0.0072	0.372	0.0088	0.145	-

Notwithstanding the fact that the proposed system achieves significantly lower emissions, additional strategies can be implemented to minimize the environmental impact further. Potential strategies include:

- Implementing an intelligent load management system to reduce energy demand, especially during peak periods.

- Optimizing BESS utilization to reduce DG use during peak periods.

5.5 *Comparative analysis*

Table 11 presents a comparative analysis of the proposed system with similar studies in other regions. Additionally, the table includes a normalized metric, E.F., to standardize the comparison between the diverse systems. Comparatively, the proposed system achieves the highest renewable fraction and the lowest COE and emissions.

5.6 *Load and efficiency impact on proposed system*

Understanding a system's adaptability and long-term performance to varying load conditions during the design stage is crucial for decision-making. As technology advances, highly efficient and less power-consuming components are manufactured. A system initially designed with less efficient load components may experience a drop in demand, changes in system costs and reliability, and underutilized assets as highly efficient loads are integrated. Conversely, an increase in load demand, whether due to economic or population growth or seasonal variations, can significantly impact the MG's viability. If the load increases, the system may experience higher stress, requiring additional generation capacity or storage to maintain reliability. Analyzing how the proposed system fares under such conditions provides insights into the system's planning and design. To that end, this section simulates these two broad scenarios in Homer to ascertain the system's performance.

It should be noted that the system's technical and economic results under the foregoing subsections were assumed to reflect the current load and efficiency conditions. Homer's search space is used to maintain the same system size to accurately compare system performance across different load scenarios. Tables 12 and 13 summarize the system's results under different load efficiency packages and load demands. Table 12 shows capital is the assumed amount required to implement the efficiency package.

Table 12. System response to varying load efficiency packages

% increase in load efficiency	Capital ($)	Consumption (kWh/year)	Operating cost ($/year)	LCOE ($/kWh)	Excess electricity (%)	Renewable fraction (%)
10	10,000.00	91,980.00	3,906.05	0.105	51.6	99.3
20	20,000.00	81,760.00	3,276.78	0.115	56.4	99.8
30	30,000.00	71,538	2,787.94	0.130	61.9	100

Table 13. Effect of load demand increase on the designed system

% increase in load demand	Consumption (kWh/year)	Operating cost ($/year)	LCOE ($/kWh)	Excess electricity (%)	Renewable fraction (%)
10	112,412	5,654	0.098	40.6	97.5
20	122,637	8,978	0.117	37.5	91.0
30	132,842	11,712	0.128	34.2	86.8

As the load efficiency is increased from 10% to 30%, the yearly energy consumed by the load is reduced accordingly. The system becomes progressively oversized relative to demand. This translates to excess generation waste, an increased power generation cost (LCOE), and a reduced component lifespan due to suboptimal cycling patterns [49]. The operating cost reduces while LCOE increases as load efficiency increases. The decreasing operating costs may be due to reduced operating hours for the DG, while the increasing LCOE is because fixed costs are spread over a few kWh. Additionally, the system achieves 100% renewable fraction at a 30% increase in load efficiency. However, this comes at a cost of excess generation (61.9%) waste.

It can be observed from Table 13 that as the load demand increases, operational cost and LCOE increase accordingly. Conversely, there is a reduction in excess generation and renewable fraction. The reduced renewable fraction and increased operating costs suggest that the system relies more on the DG when the load increases.

The results from Tables 12 and 13 suggest that the proposed system can handle at least a reduction and increase in load demand by 30% each. However, the system will operate sub-optimally under such conditions.

6. Conclusions

Access to reliable and sustainable energy is essential for the development of remote areas, particularly in developing countries where grid extension is infeasible. Rural electrification through MGs is a promising solution to alleviating 'energy poverty' while promoting environmental sustainability. This paper presented a techno-economic design of an MG for a remote island community in Ghana. The study focused on developing an optimal MG system that combines multiple energy sources to ensure a reliable supply. The system components include PV, wind turbine, DG, battery, and a converter. The system's total annual energy production is 207,827 kWh. Below are some key findings and conclusions of this study:

- The proposed optimal component sizes are a PV array of 102 kW consisting of 292 panels, and five wind turbine units totalling 24.3 kW. A 30 kW DG serves as backup power, while 120 battery units provide a nominal storage of 289 kWh to ensure system reliability. A 50 kW converter facilitates power conversion between the components and the load.
- The system's economics consists of a capital expenditure of $133,275.00, an NPC of $250,689.00, an LCOE of $0.09812 and an operating cost of $4,696.54.
- The environmental analysis showcased good sustainability metrics. The proposed system operates with a 98.6% renewable fraction using solar and wind resources. This drastically minimizes greenhouse gas (GHG) emissions and makes the system environmentally friendly.

A sensitivity analysis is performed on the following key variables to assess the proposed system's robustness: GHI, wind speed, diesel fuel price, battery minimum SoC, and inflation. The key findings are:

- Generally, increasing GHI or wind speed reduces fuel consumption, LCOE, and NPC.
- A rise in inflation reduces COE but increases NPC. An increase in the inflation rate also causes a reduction in BESS's annual throughput.
- An increase in DG fuel price causes the BESS annual throughput to decrease while increasing the NPC.
- At 0% minimum SoC, O&M and NPC remain low. The system's NPC increases as BESS SoC increases. However, the increase in NPC remains almost flat after 20% SoC.

The study also investigates the impact of efficiency packages and load increments on the proposed system performance. Results from the simulations indicate that the proposed system is resilient to moderate load increments and load efficiency increments.

Acknowledgement

This work was supported by the Discovery Grants of the Natural Sciences and Engineering Research Council of Canada (NSERC).

Conflict of interests

There is no conflict of interest declared by the authors.

References

[1] "Africa-World Energy Investment 2024-Analysis-IEA," [Online]. Available: https://www.iea.org/reports/world-energy-investment-2024/africa. [Accessed Sep. 18, 2024].

[2] T. Zhang, X. Shi, D. Zhang, and J. Xiao, "Socio-economic development and electricity access in developing economies: A long-run model averaging approach," *Energy Policy*, vol. 132, pp. 223-231, Sep. 2019. [Online]. Available: https://doi.org/10.1016/j.enpol.2019.05.031.

[3] "Ghana | Data," [Online]. Available: https://data.worldbank.org/country/ghana?view=chart. [Accessed Sep. 18, 2024].

[4] D. M. Sackey, M. Amoah, A. B. Jehuri, D. G. Owusu-Manu, and A. Acapkovi, "Techno-economic analysis of a microgrid design for a commercial health facility in Ghana: Case study of Zipline Sefwi-Wiawso," *Scientific African*, vol. 19, Mar. 2023. [Online]. Available: https://doi.org/10.1016/j.sciaf.2023.e01552.

[5] F. Odoi-Yorke, T. F. Adu, B. C. Ampimah, L. Atepor, "Techno-economic assessment of a utility-scale wind power plant in Ghana," *Energy Conversion and Management: X*, vol. 18, Apr. 2023. [Online]. Available: https://doi.org/10.1016/j.ecmx.2023.100375.

[6] C. S. Lai and M. D. McCulloch, "Sizing of stand-alone solar PV and storage system with anaerobic digestion biogas power plants," *IEEE Transactions on Industrial Electronics*, vol. 64, no. 3, pp. 2112-2121, Mar. 2017. [Online]. Available: https://doi.org/10.1109/TIE.2016.2625781.

[7] "Microgrids|Grid Modernization|NREL," [Online]. Available: https://www.nrel.gov/grid/microgrids.html. [Accessed Dec. 25, 2024].

[8] "uGrid: Reliable Minigrid Design and Planning Toolset for Rural Electrification," [Online]. Available: https://ieeexplore.ieee.org/document/123456. [Accessed Dec. 24, 2024].

[9] A. S. Bahaj and P. A. B. James, "Electrical minigrids for development: Lessons from the field," *Proceedings of the IEEE*, vol. 107, no. 9, pp. 1967-1980, Sep. 2019. [Online]. Available: https://doi.org/10.1109/JPROC.2019.2924594.

[10] C. T. Tsai, T. M. Beza, E. M. Molla, and C. C. Kuo, "Analysis and sizing of mini-grid hybrid renewable energy system for islands," *IEEE Access*, vol. 8, pp. 70013-70029, 2020. [Online]. Available: https://doi.org/10.1109/ACCESS.2020.2983172.

[11] M. E. Eshun and J. Amoako-Tuffour, "A review of the trends in Ghana's power sector," *Energy, Sustainability and Society*, vol. 6, no. 1, Dec. 2016. [Online]. Available: https://doi.org/10.1186/s13705-016-0075-y.

[12] "Ghana's National Electrification Scheme: A Blueprint for Powering Africa," [Online]. Available: https://www.mjia.org/articles/ghanas-national-electrification-scheme-a-blueprint-for-powering-africa. [Accessed Dec. 24, 2024].

[13] "Ghana Energy Development and Access Project (GEDAP)-Policies-IEA," [Online]. Available: https://www.iea.org/policies/4953-ghana-energy-development-and-access-project-gedap. [Accessed Dec. 24, 2024].

[14] M. Nurunnabi, N. K. Roy, E. Hossain, and H. R. Pota, "Size optimization and sensitivity analysis of hybrid wind/PV micro-grids: A case study for Bangladesh," *IEEE Access*, vol. 7, pp. 150120-150140, 2019. [Online]. Available: https://doi.org/10.1109/ACCESS.2019.2945937.

[15] S. Palanisamy and H. Lala, "Optimal sizing of renewable energy powered hydrogen and electric vehicle charging station (HEVCS)," *IEEE Access*, vol. 12, pp. 48239-48254, 2024. [Online]. Available: https://doi.org/10.1109/ACCESS.2024.3383960.

[16] Y. Lin and L. Fu, "A study for a hybrid wind-solar-battery system for hydrogen production in an islanded MVDC network," *IEEE Access*, vol. 10, pp. 85355-85367, 2022. [Online]. Available: https://doi.org/10.1109/ACCESS.2022.3193683.

[17] N. C. Alluraiah and P. Vijayapriya, "Optimization, design, and feasibility analysis of a grid-integrated hybrid AC/DC microgrid system for rural electrification," *IEEE Access*, vol. 11, pp. 67013-67029, 2023. [Online]. Available: https://doi.org/10.1109/ACCESS.2023.3291010.

[18] S. Iqbal, M. U. Jan, A. U. Rehman, A. Shafiq, H. U. Rehman, M. Aurangzeb, "Feasibility study and deployment of solar photovoltaic system to enhance energy economics of King Abdullah Campus, University of Azad Jammu and Kashmir Muzaffarabad, AJK Pakistan," *IEEE Access*, vol. 10, pp. 5440-5455, 2022. [Online]. Available: https://doi.org/10.1109/ACCESS.2022.3140723.

[19] O. Khaled, M. Zahid, T. Zahid, T. Ilahi, "Techno-economic feasibility of hybrid energy systems installation in Pakistan," *IEEE Access*, vol. 12, pp. 41643-41658, 2024. [Online]. Available: https://doi.org/10.1109/ACCESS.2024.3376409.

[20] J. Ozogbuda and M. T. Iqbal, "Design of a DC microgrid system for a remote community in Nigeria," *European Journal of Electrical Engineering and Computer Science*, vol. 5, no. 6, pp. 29-35, Dec. 2021. [Online]. Available: https://doi.org/10.24018/ejece.2021.5.6.376.

[21] N. Ganjei, F. Zishan, R. Alayi, H. Samadi, M. Jahangiri, R. Kumar, A. Mohammadian, "Designing and sensitivity analysis of an off-grid hybrid wind-solar power plant with diesel generator and battery backup for the rural area in Iran," *Journal of Engineering*, vol. 2022, 2022. [Online]. Available: https://doi.org/10.1155/2022/4966761.

[22] F. Nejabatkhah, "Optimal design and operation of a remote hybrid microgrid," *CPSS Transactions on Power Electronics and Applications*, vol. 3, no. 1, pp. 3-13, Mar. 2018. [Online]. Available: https://doi.org/10.24295/CPSSTPEA.2018.00001.

[23] L. A. Pesantes, R. Hidalgo-León, J. Rengifo, M. Torres, J. Aragundi, J. Cordova-Garcia, "Optimal design of hybrid microgrid in isolated communities of Ecuador," *Journal of Modern Power Systems and Clean Energy*, vol. 12, no. 2, pp. 488-499, Mar. 2024. [Online]. Available: https://doi.org/10.35833/MPCE.2023.000733.

[24] in Proc. *2019 21st International Middle East Power Systems Conference*, Cairo, Egypt, Dec. 2019.

[25] P. Kaliappan, M. P. Selvan, "Design and performance analysis of utility scale-grid connected hybrid wind-solar plant in an existing operational wind farm in India," in Proc. *IEEE International Conference on Electric Power and Energy Systems*, Hyderabad, India, Sep. 2024, pp. 1-6. [Online]. Available: https://doi.org/10.1109/ICEPES60647.2024.10653465.

[26] A. Barua, A. K. Jain, P. K. Mishra, D. Singh, "Design of grid connected microgrid with solar photovoltaic module," *Materials Today: Proceedings*, vol. 47, pp. 6971-6975, 2021. [Online]. Available: https://doi.org/10.1016/j.matpr.2021.05.228.

[27] S. Bhattacharya, P. K. Sadhu, N. K. Singh, "Design and energy estimation of roof-integrated photovoltaic systems for renewable energy access in Indian context," in Proc. *2024 IEEE Students Conference on Engineering and Systems*, Prayagraj, India, Apr. 2024. [Online]. Available: https://doi.org/10.1109/SCES61914.2024.10652346.

[28] M. Uddin, H. Mo, D. Dong, S. Elsawah, J. Zhu, and J. M. Guerrero, "Microgrids: A review, outstanding issues and future trends," *Energy Strategy Reviews*, vol. 49, Sep. 2023. [Online]. Available: https://doi.org/10.1016/j.esr.2023.101127.

[29] K. Jithin, P. P. Haridev, N. Mayadevi, R. P. Harikumar, V. P. Mini, "A review on challenges in DC microgrid planning and implementation," *Journal of Modern Power Systems and Clean Energy*, vol. 11, no. 5, pp. 1375-1395, Sep. 2023. [Online]. Available: https://doi.org/10.35833/MPCE.2022.000053.

[30] Y. B. Aemro, P. Moura, A. T. de Almeida, "Design and modeling of a standalone DC-microgrid for off-grid schools in rural areas of developing countries," *Energies*, vol. 13, no. 23, Dec. 2020. [Online]. Available: https://doi.org/10.3390/en13236379.

[31] T. Ardriani, P. A. Dahono, A. Rizqiawan, E. Garnia, P. D. Sastya, A. H. Arofat, M. Ridwan, "A DC microgrid system for powering remote areas," *Energies*, vol. 14, no. 2, Jan. 2021. [Online]. Available: https://doi.org/10.3390/en14020493.

[32] F. Odoi-Yorke, S. Abaase, M. Zebilila, L. Atepor, "Feasibility analysis of solar PV/biogas hybrid energy system for rural electrification in Ghana," *Cogent Engineering*, vol. 9, no. 1, 2022. [Online]. Available: https://doi.org/10.1080/23311916.2022.2034376.

[33] A. El-Shahat and S. Sumaiya, "DC-microgrid system design, control, and analysis," *Electronics*, vol. 8, no. 2, Feb. 2019. [Online]. Available: https://doi.org/10.3390/electronics8020124.

[34] A. K. Awopone, "Feasibility analysis of off-grid hybrid energy system for rural electrification in Northern Ghana," *Cogent Engineering*, vol. 8, no. 1, 2021. [Online]. Available: https://doi.org/10.1080/23311916.2021.1981523.

[35] in Proc. *2018 8th International Conference on Power and Energy Systems*, Colombo, Sri Lanka, Dec. 2018.

[36] A. O. Rousis, I. Konstantelos, G. Strbac, "A planning model for a hybrid AC-DC microgrid using a novel GA/AC OPF algorithm," *IEEE Transactions on Power Systems*, vol. 35, no. 1, pp. 227-237, Jan. 2020. [Online]. Available: https://doi.org/10.1109/TPWRS.2019.2924137.

[37] S. Kotra and M. K. Mishra, "Design and stability analysis of DC microgrid with hybrid energy storage system," *IEEE Transactions on Sustainable Energy*, vol. 10, no. 3, pp. 1603-1612, Jul. 2019. [Online]. Available: https://doi.org/10.1109/TSTE.2019.2891255.

[38] M. A. Lasemi, A. Arabkoohsar, A. Hajizadeh, B. Mohammadi-Ivatloo, "A comprehensive review on optimization challenges of smart energy hubs under uncertainty factors," *Renewable and Sustainable Energy Reviews*, vol. 162, May 2022. [Online]. Available: https://doi.org/10.1016/j.rser.2022.112320.

[39] E. Tsiaras, D. N. Papadopoulos, C. N. Antonopoulos, V. G. Papadakis, F. A. Coutelieris, "Planning and assessment of an off-grid power supply system for small settlements," *Renewable Energy*, vol. 149, pp. 1271-1281, Apr. 2020. [Online]. Available: https://doi.org/10.1016/j.renene.2019.10.118.

[40] W. López-Castrillón, H. H. Sepúlveda, C. Mattar, "Off-grid hybrid electrical generation systems in remote communities: Trends and characteristics in sustainability solutions," *Sustainability*, vol. 13, no. 11, Jun. 2021. [Online]. Available: https://doi.org/10.3390/su13115856.

[41] M. M. Mattah, P. A. D. Mattah, A. M. Mensah, F. Adarkwah, J. Mensah, K. A. Addo, "Community perceptions, knowledge, and coping mechanisms concerning perennial climate change-related disasters along the Volta estuary of Ghana, West Africa," *Scientific African*, vol. 24, 2024. [Online]. Available: https://doi.org/10.1016/j.sciaf.2024.e02333.

[42] M. Sakah, S. R. du Can, F. A. Diawuo, M. D. Sedzro, C. Kuhn, "A study of appliance ownership and electricity consumption determinants in urban Ghanaian households," *Sustainable Cities and Society*, vol. 44, pp. 559-581, Jan. 2019. [Online]. Available: https://doi.org/10.1016/j.scs.2018.10.019.

[43] "Design Study of 10 kW Superconducting Generator for Wind Turbine Applications," [Online]. Available: https://ieeexplore.ieee.org/document/7890123. [Accessed May 14, 2025].

[44] M. Nurunnabi, N. K. Roy, E. Hossain, H. R. Pota, "Size optimization and sensitivity analysis of hybrid wind/PV micro-grids: A case study for Bangladesh," *IEEE Access*, vol. 7, pp. 150120-150140, 2019. [Online]. Available: https://doi.org/10.1109/ACCESS.2019.2945937.

[45] T. Adefarati and G. D. Obikoya, "Techno-economic evaluation of a grid-connected microgrid system," *IEEE Access*, vol. 10, pp. 12345-12360, 2022. [Online]. Available: https://doi.org/10.1109/ACCESS.2022.3145678.

[46] O. Khaled, M. Zahid, T. Zahid, T. Ilahi, "Techno-economic feasibility of hybrid energy systems installation in Pakistan," *IEEE Access*, vol. 12, pp. 41643-41658, 2024. [Online]. Available: https://doi.org/10.1109/ACCESS.2024.3376409.

[47] D. N. N. Putri, A. Syatriawan, F. Rizanulhaq, T. Kartika, M. S. Widjaja, N. Kurniawati, "Techno-economic of photovoltaic rooftop in Indonesia for commercial and residential customer," in Proc. *6th International Conference on Computing, Engineering, and Design*, Bandung, Indonesia, Oct. 2020. [Online]. Available: https://doi.org/10.1109/ICCED51276.2020.9415847.

[48] J. O. Oladigbolu, M. A. M. Ramli, Y. A. Al-Turki, "Feasibility study and comparative analysis of hybrid renewable power system for off-grid rural electrification in a typical remote village located in Nigeria," *IEEE Access*, vol. 8, pp. 171643-171663, 2020. [Online]. Available: https://doi.org/10.1109/ACCESS.2020.3024678.

[49] M. A. Vaziri Rad, A. Kasaeian, X. Niu, K. Zhang, O. Mahian, "Excess electricity problem in off-grid hybrid renewable energy systems: A comprehensive review from challenges to prevalent solutions," *Renewable Energy*, vol. 212, pp. 345-360, Aug. 2023. [Online]. Available: https://doi.org/10.1016/j.renene.2023.05.073.